

Quinoxalines XIV.[†] Synthesis, ¹H, ¹³C, ¹⁵N NMR spectroscopic, and quantum chemical study of 1*H*-pyrazolo[3,4-*b*]quinoxalines (flavazoles)

Matthias Heydenreich, Andreas Koch, Gerhard Sarodnick and Erich Kleinpeter*

Department of Chemistry, University of Potsdam, PO Box 69 15 53, D-14415 Potsdam, Germany

Received 25 October 2004; revised 15 December 2004; accepted 7 January 2005

Available online 27 January 2005

Abstract—The synthesis of a series of 1*H*-pyrazolo[3,4-*b*]quinoxalines (flavazoles) by acylation, alkylation, halogenation, and aminomethylation of the parent compound is reported and their structure is investigated by ¹H, ¹³C, and ¹⁵N NMR spectroscopy. The restricted rotation about the partial C, N double bond of the *N*-acyl derivatives **7–10** is studied by dynamic NMR spectroscopy and the barriers to rotation are determined. In order to assign unequivocally the ¹⁵N chemical shifts of N-4 and N-9, in case of 3-substituted flavazoles, exemplary the ¹H, ¹³C, and ¹⁵N NMR chemical shifts of **34**, **35**, and **39** are also theoretically calculated by quantum chemical methods [ab initio at different levels of theory (HF/6-31G* and B3LYP/6-31G*)].

© 2005 Elsevier Ltd. All rights reserved.

1. Introduction

Previously, we reported a new and convenient synthesis of 1*H*-pyrazolo[3,4-*b*]quinoxalines (flavazoles) by reacting quinoxaline-2-aldoximes and -ketoximes with hydrazine, alkylhydrazines or arylhydrazines under acidic conditions to afford unsubstituted, 1- and/or 3-substituted flavazoles; various other substituents could be introduced by acylation and alkylation of the 1-unsubstituted compounds.²

It is the major objective of the present paper to continue these studies and to further investigate substitution possibilities by acylation, alkylation, halogenation, and Mannich reaction. Beside synthesis, NMR spectroscopic properties of the flavazoles (cf. Fig. 1) were studied in detail

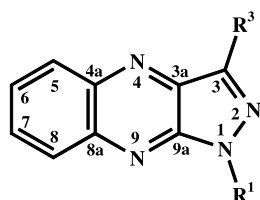


Figure 1. Investigated 1*H*-pyrazolo[3,4-*b*]quinoxalines (flavazoles) (**1–48**), R¹ and R³ are given in Schemes 1–4.

Keywords: 1*H*-Pyrazolo[3,4-*b*]quinoxalines; Flavazoles; Restricted rotation; Dynamic NMR; Theoretical calculations.

[†] See Ref. 1.

* Corresponding author. Tel.: +49 331 9775210; fax: +49 331 9775064; e-mail: kp@chem.uni-potsdam.de

by employing the whole arsenal of 1D and 2D NMR spectroscopy and also theoretical methods. The restricted rotation about the exocyclic partial C, N double bond in the *N*-acyl compounds **7**, **8**, **9**, and **10**, respectively, was studied by dynamic NMR.

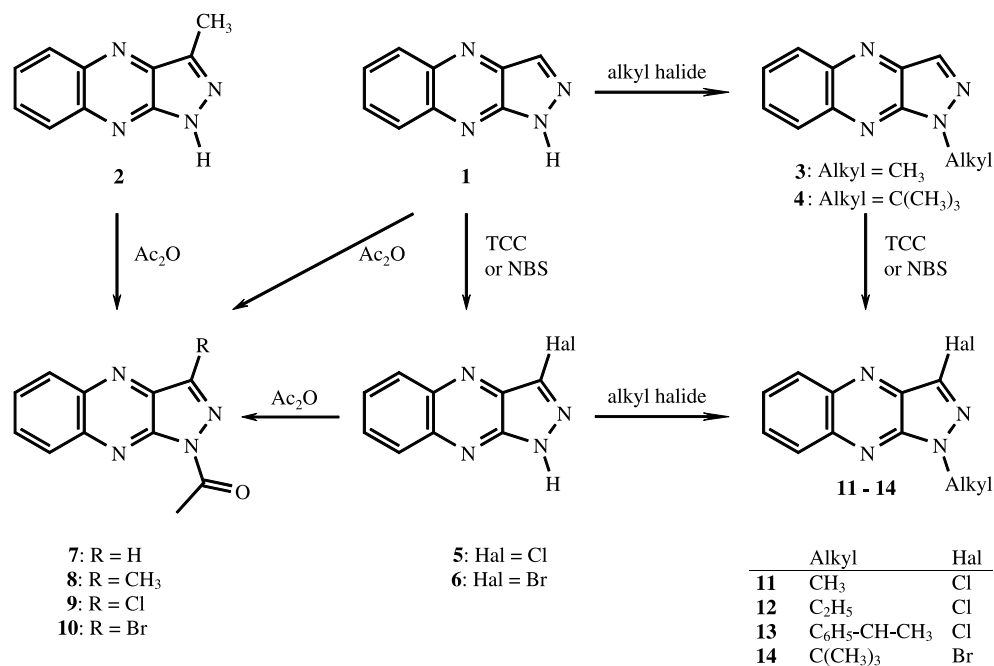
2. Results and discussion

2.1. Syntheses

1*H*-Pyrazolo[3,4-*b*]quinoxalines were acylated only in position 1 by applying aroyl chlorides in the presence of pyridine.² When employing acetic anhydride instead, also the nonsubstituted flavazole (**1**), the 3-methyl substituted analogue **2**, and the 3-chloro- and 3-bromo-substituted compounds (**5** and **6**), could be acylated. If acetic anhydride is applied in 25-fold excess and as solvent too, **7–10** could be also obtained (cf. Scheme 1).

1*H*-Pyrazolo[3,4-*b*]quinoxaline (**1**) can be readily halogenated, but the reaction product proved to be dependent on the substituent pattern: nonsubstituted flavazole is halogenated in position 3, thus, with trichloroisocyanuric acid (TCC) 3-chloro-1*H*-pyrazolo[3,4-*b*]quinoxaline (**5**) was obtained which is described as cytotoxic and was already synthesized from 3-amino-1*H*-pyrazolo[3,4-*b*]quinoxaline.³ The reaction of **1** with *N*-bromosuccinimide yielded 3-bromo-1*H*-pyrazolo[3,4-*b*]quinoxaline (**6**).

The 3-halogeno substituted reaction products **5** and **6** can be



Scheme 1.

further acylated and alkylated in position 1; thus, the reaction of **5** with methyl iodide yielded 3-chloro-1-methyl-1*H*-pyrazolo[3,4-*b*]quinoxaline (**11**), with ethyl iodide 3-chloro-1-ethyl-1*H*-pyrazolo[3,4-*b*]quinoxaline (**12**) was obtained and with 1-bromo-1-phenylethane the corresponding 3-chloro-1-(1-phenylethyl)-1*H*-pyrazolo[3,4-*b*]quinoxaline (**13**) was synthesized (cf. Scheme 1).

As seen in Scheme 1 there is a second path of reaction from the nonsubstituted flavazole (**1**) to the 1-alkyl-3-halogeno-1*H*-pyrazolo[3,4-*b*]quinoxalines via the alkyl substituted derivatives (e.g., **3**, **4**): first, **1** is alkylated to **3** and, then, chlorinated employing TCC. Along this path, the methyl group remains in the molecule and the reaction product **11** obtained proved to be identical to the reaction product of the

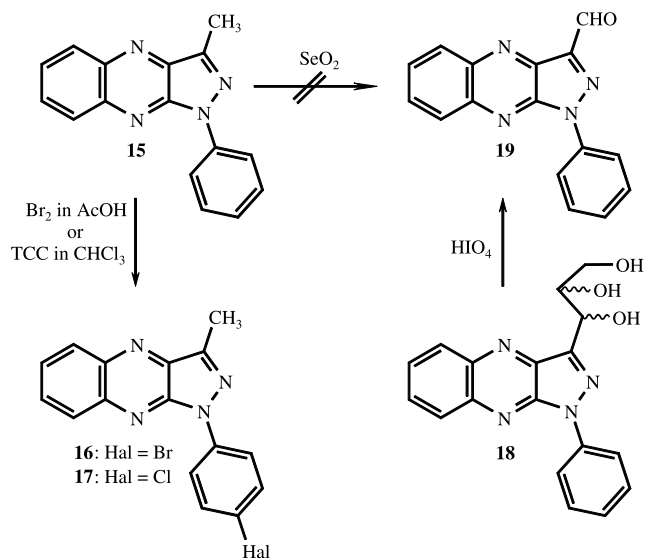
alkylation reaction of **5**. Similarly, halogenation of 1-*tert*-butyl-1*H*-pyrazolo[3,4-*b*]quinoxaline (**4**) with NBS led to 3-bromo-1-*tert*-butyl-1*H*-pyrazolo[3,4-*b*]quinoxaline (**14**).

The halogenation of 3-methylflavazole (**2**) and 1,3-dimethylflavazole (**33**) under the same conditions was useless, the unsuccessful bromination of **15** (cf. Scheme 2) was already reported previously.⁴ However, if elemental bromine in glacial acetic acid at room temperature is used, the *p*-substituted product **16** could be isolated. The corresponding chloro compound **17** could be synthesized with TCC. **17** was already obtained from the reaction of 2-acetylquinoxaline oxime with 4-chlorophenylhydrazine.²

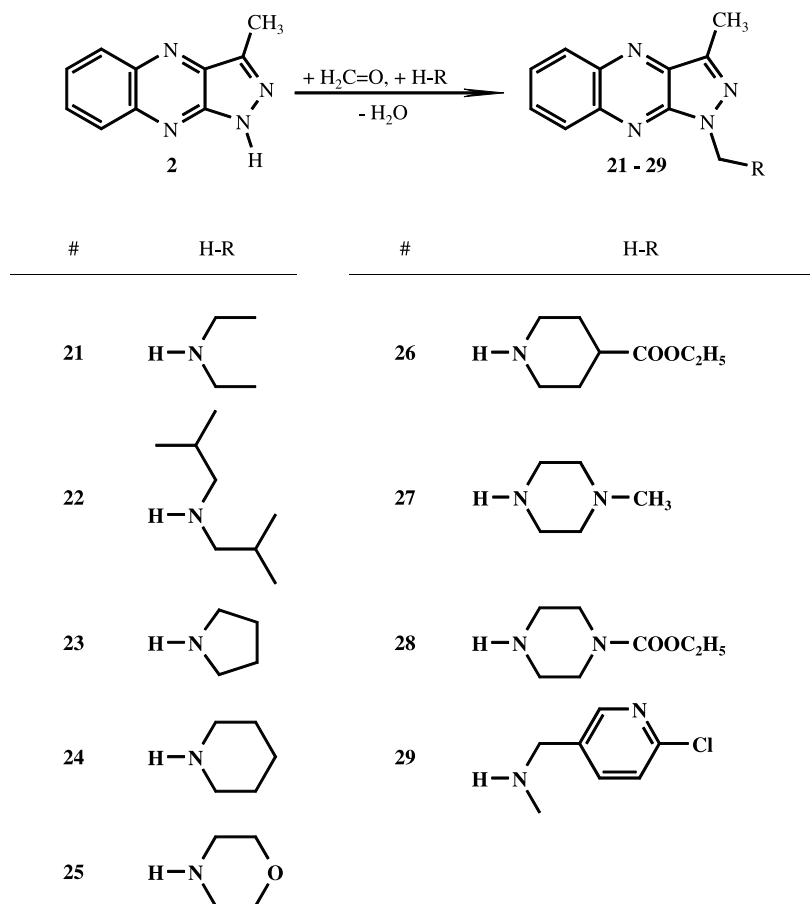
Generally, the chemical reactivity of the methyl group in position 3 of the 1*H*-pyrazolo[3,4-*b*]quinoxalines proved to be very weak. Experiments to oxidize **15** by KMnO₄, CrO₃, SeO₂, and CrO₂Cl₂ were unsuccessful.⁴ Otherwise, El-Maghraby et al. report the oxidation of **15** with SeO₂ in ethanol to the corresponding aldehyde.⁵ This procedure could not be reproduced in our investigations, even when replacing ethanol by other solvents as dioxane/water, toluene, xylene, mesitylene, diethyleneglycol diethylether, or at their reflux temperature. On the other hand, 1-phenyl-1*H*-pyrazolo[3,4-*b*]quinoxalin-3-carbaldehyde (**19**)⁶ can be synthesized by oxidation of 1-phenyl-3-(*D*-erythro-tri-hydroxypropyl)-1*H*-pyrazolo[3,4-*b*]quinoxaline (**18**) with potassium periodate.⁷

The aldehyde **19** reacted with *p*-toluenesulfonyl hydrazide giving the corresponding tosylhydrazone **20**.

Also the Mannich reaction of 3-methyl flavazoles was studied: the electron withdrawing effect of the nitrogen atoms in the 1*H*-pyrazolo[3,4-*b*]quinoxaline ring system should accelerate the elimination of the proton and, thus, from 3-methyl-1*H*-pyrazolo[3,4-*b*]quinoxaline (**2**) with



Scheme 2.



Scheme 3.

formaldehyde and a number of different secondary amines the corresponding Mannich bases (**21–29**) were synthesized in mostly good or very good yields (cf. Scheme 3).

2.2. General assignment of the chemical shifts and coupling constants

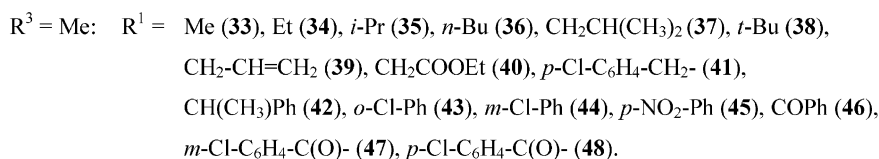
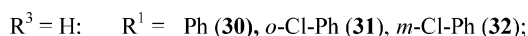
For NMR analysis additional compounds (**30–48**) were taken into account for which the syntheses were already described in a previous paper.² Their substitution pattern is given in Scheme 4.

The unequivocal assignment of the chemical shifts of both proton and carbon atoms of the pyrazole ring of the compounds **1–4**, **7**, and **30–32** proved unequivocal. The HMQC and HMBC experiments (starting from $R^3=H$) show all connectivities which are needed to assign also nitrogen chemical shifts. To get an impression about the value of the long-range coupling constants selective long-

range⁸ and J -HMBC-1⁹ experiments for ${}^nJ(C,H)$ and J -HMBC-2 experiments⁹ for ${}^nJ(N,H)$ were proceeded exemplary at compound **4**. The corresponding values thus obtained are given in Table 1.

The difference in the value of ${}^2J(C-3a, H-3)$ between the two experiments may be due to a relatively bad digital resolution of about 3.6 Hz in the J -HMBC-1 experiment. Recently it was shown that both experiments agree well.¹⁰

In cases where $R^3=CH_3$ or CHO, long-range connectivities from the corresponding substituent protons to C-3a, N-2, and N-1, respectively, were used to assign unequivocally the latter chemical shifts. The chemical shift of C-9a was then assigned by long-range connectivities to substituent protons in R^1 , or, if this was not possible, using the rule that this carbon is the only one in the whole molecule who gives no HMBC signals to any of the hydrogen atoms. To know something about the long-range coupling constants ${}^nJ(C, H)$



Scheme 4.

Table 1. Long-range coupling constants in compound **4** (Hz); signs not estimated

$^nJ(\text{X,H})$	N-1, <i>t</i> -Bu	N-1, H-3	N-4, H-3	N-4, H-5	N-9, H-8	C-3a, H-3	C-4a, H-6	C-4a, H-8	C-5, H-7	C-6, H-8	C-7, H-5	C-8, H-5	C-8, H-6	C-8a, H-5	C-8a, H-7	C-9a, H-3
Sellr ^a						10.0					9.5	1.8		5.5		3.7
HMBC ^b	2.4	6.6	13.4	1.1	1.2	13.4	9.9	5.1	7.4	9.4	9.4	≈0	7.5	5.1	9.9	3.4

^a Selective long-range experiment according to Ref. 8. Not all possible long-range couplings were determined; only two hydrogens (H-3 and H-5) were selected for irradiation.

^b *J*-HMBC experiments according to Ref. 9.

in these compounds exemplary a *J*-HMBC-2 experiment on compound **40** was carried out. The detected coupling constants are given in Table 2.

The compounds **9–14** contain no protons in position 3, therefore, the corresponding long-range couplings cannot be taken to assign unequivocally C-3a. Here, the assignments given in Table 3 are in analogy with the other compounds studied.

The chemical shifts of N-4 and N-9 were assigned by HMBC measurements corroborated by theoretical calculations (vide infra). Each of them were found for the compounds studied in a relatively narrow range (−67 to −57 ppm for N-4, and −116.6 to −97.5 ppm for N-9). These two absorption ranges are considered to be large enough to assign the two ¹⁵N chemical shifts unequivocally. These different chemical shifts of the nitrogen atoms N-4 and N-9 are thus the key to assign the chemical shifts of the phenylene ring atoms. The long-range connectivities in the H,N-HMBC from H-5 to N-4 and H-8 to N-9 are marking the beginning and the end of the four-spin system H-5–H-8, which can be assigned unequivocally furthermore by H,H-COSY experiments. Direct C–H correlation NMR experiments (HMQC) yield the ¹³C chemical shifts of C-5–C-8, and the corresponding values of C-4a and C-8a are accessible via long-range connectivities from the H,C-HMBC spectra.

2.2.1. ¹H NMR chemical shifts. The experimentally detected ¹H NMR chemical shifts of the investigated compounds are given in Table 3.

In the compounds **1, 3, 4, 7, and 30–32** (cf. Tables 3 and 4) position 3 is unsubstituted: the H-3 protons were found to be in the range of 8.40–8.79 ppm. All attempts to correlate their chemical shifts with electronic substituent parameters (σ_m , σ_p , σ_I , and σ_R , respectively) failed. In cases of R³=Me the range of the chemical shifts of the methyl protons was determined to be even more narrow (2.66–2.89 ppm). An influence of the different substituents in R¹ is again not perceptible.

The ranges of the chemical shifts of the phenylene protons are as follows: 8.03–8.35 ppm for H-5, 7.52–7.91 ppm for H-6, 7.60–7.98 ppm for H-7, and 7.92–8.35 ppm for H-8, respectively. In all compounds having no carbonyl function directly bound to positions 1 or 3, H-5 is always downfield with respect to H-8, and H-6 is upfield with respect to H-7 (with the exception of **31**: here is $\delta[\text{H-6}] \approx \delta[\text{H-7}]$). Introducing an aldehyde group into position 3 (**19**) reverses this rule. Carbonyl functions at position 1 reduce at least the difference between H-5 and H-8 (**47**) up to zero (**9, 10**) or even below zero (**7, 8, 46, 48**). As to H-6 and H-7 of the carbonyl containing compounds, however, they follow (with the exception of **19**) the rule given above.

Table 2. Long-range C,H coupling constants as determined in compound **40** (Hz); sign not estimated

	CH ₃ –CH ₂	CH ₂ –CH ₃	CH ₂ –OCO	CH ₃ –C-3a	CH ₃ –C-3	CH ₂ –C-9a	CH ₂ –CO
$^nJ(\text{C,H})$	4.2	2.1	2.6	2.7	7.2	2.1	5.4

Table 3. ¹H NMR chemical shifts (ppm) and H,H-coupling constants (Hz) of some selected compounds studied

Compound	R ¹	R ³	5	6	7	8
1	14.15 (br)	8.79 (s)	8.27 (d, 8.0)	7.86 (t, 8.3)	7.95 (t, 8.3)	8.18 (d, 8.5)
2	11.23 (br)	2.85 (s)	8.32 (d, 8.6)	7.76 (t, 8.3)	7.87 (t, 8.3)	8.19 (d, 8.5)
3	4.18 (s)	8.40 (s)	8.13 (d, 8.5)	7.63 (t, 8.3)	7.73 (t, 8.5)	8.01 (d, 8.6)
4	1.92 (s)	8.43 (s)	8.15 (d, 8.3)	7.63 (t, 8.2)	7.70 (t, 8.5)	8.09 (d, 8.5)
7	2.94 (s)	8.56 (s)	8.17 (d, 8.4)	7.80 (t, 8.3)	7.88 (t, 8.4)	8.25 (d, 8.7)
9	2.93 (s)	–	8.35 (d, 8.5)	7.91 (t, 8.2)	7.98 (t, 8.4)	8.35 (d, 8.5)
15	<i>o</i> : 8.30 (d, 8.3); <i>m</i> : 7.44 (t, 8.6); <i>p</i> : 7.20 (t, 8.3)	2.72 (s)	8.03 (d, 8.5)	7.52 (t, 8.3)	7.60 (t, 8.5)	7.92 (d, 8.5)
19	<i>o</i> : 8.35 (m); <i>m</i> : 7.53 (t, 7.4); <i>p</i> : 7.36 (t, 7.4)	10.38 (s)	8.05 (d, 8.7)	7.81 (t, 8.3)	7.75 (t, 8.3)	8.35 (m)
30	<i>o</i> : 8.37 (d, 8.7); <i>m</i> : 7.50 (t, 8.5); <i>p</i> : 7.27 (t, 7.4)	8.54 (s)	8.12 (d, 8.3)	7.63 (t, 8.5)	7.71 (t, 8.3)	8.06 (d, 8.7)
33	4.01 (s)	2.66 (s)	8.04 (d, 8.6)	7.54 (t, 7.7)	7.64 (t, 8.0)	7.89 (d, 8.6)
34	4.53 (q, 7.3); 1.56 (t, 7.3)	2.75 (s)	8.12 (d, 8.6)	7.58 (t, 8.0)	7.68 (t, 8.3)	7.98 (d, 8.5)
40	5.30 (s); 4.22 (q, 7.2); 1.23 (t, 7.2)	2.80 (s)	8.23 (d, 8.5)	7.67 (t, 8.3)	7.76 (t, 8.4)	8.06 (d, 8.7)
47	4', 5': 7.50 (m); 6': 7.44 (m); 7': 7.64 (d, 7.0)	2.74 (s)	8.26 (d, 8.1)	7.83 (t, 8.2)	7.89 (t, 8.3)	8.25 (d, 8.1)

A complete table containing data of all measured compounds is included in the Supplementary material.

Table 4. ^{13}C and ^{15}N NMR chemical shifts (ppm) of some of the selected compounds studied

Compound	1	2	3	3a	4	4a	5	6	7	8	8a	9	9a	Others
1	−202.0 $^1J_{\text{N,H}}$: 106.7 Hz	−42.6	134.4	136.4	−62.9	140.6	129.9	127.8	130.8	128.4	141.0	−113.4	143.1	
2	−209.5 $^1J_{\text{N,H}}$: 105.8 Hz	−51.8	144.7	136.6	−64.7	141.0	130.4	127.8	131.1	128.2	141.3	−114.5	144.0	CH ₃ : 11.8
3	−210.2	−37.8	132.8	136.4	−63.0	140.8	129.9	127.3	130.3	128.3	141.2	−114.3	141.7	CH ₃ : 33.9
4	−182.8	−39.7	131.6	137.3	−67.0	140.4	129.7 ^a	127.2	129.8 ^a	128.9	140.6	−106.7	142.0	<i>t</i> -Bu: 60.5; 28.8
7	−167.2	−45.2	141.5	138.1	−60.0	141.5	129.8	129.3	131.5	129.3	141.3	−99.5	142.6	C=O: 168.1; CH ₃ : 23.5
9	−172.0	−60.7	140.9	134.4	−64.3	142.1	130.4	130.4	132.7	129.7	142.5	−97.9	143.4	COCH ₃ : 167.6; 23.7
15	−198.8	−52.8	143.9	137.3	−63.5	140.2	129.8	127.5	130.4	128.7	141.0	−109.8	142.0	CH ₃ : 11.5; <i>i</i> : 129.2; <i>o</i> : 119.0; <i>m</i> : 128.8; <i>p</i> : 124.9
19	−185.8	−29.4	140.7	134.1	−59.0	142.4	130.3	129.3	131.5	128.8	140.7	−103.7	142.2	CHO: 184.3; <i>i</i> : 138.0; <i>o</i> : 120. 2; <i>m</i> : 129.0; <i>p</i> : 127.0
30	−192.4	−44.2	135.0	137.8	−62.7	141.1	130.0	128.2	130.8	129.0	141.3	−108.5	141.7	<i>i</i> : 139.2; <i>o</i> : 119.7; <i>m</i> : 129.0; <i>p</i> : 125.7
33	−217.9	−46.0	141.3	135.5	−63.7	139.8	129.8	126.5	129.9	127.9	140.9	−116.3	142.1	CH ₃ : 11.2; NCH ₃ : 33.2
34	−204.2	−48.7	141.5	136.0	−64.1	140.2	129.9	126.6	130.0	128.1	141.1	−116.6	141.9	CH ₃ : 11.4; Et: 41.6; 14.5
40	−217.2	−47.6	143.6	136.5	−62.3	140.8	130.2	127.3	130.6	128.3	141.5	−115.9	143.3	CH ₃ : 11.6; 1': 47.9; 2': 167.9; 3': 61.6; 4': 14.0
47	−172.9	−53.8	149.8	138.6	−60.3	141.5	130.0	131.5	129.5	129.6	141.7	−98.1	143.8	CH ₃ : 11.7; C=O: 164.6; 1': 134.4; 2': 131.7; 3': 129.5; 4': 131.6; 5': 126.6; 6': 129.3

A complete table containing data of all measured compounds is included in the Supplementary material.

^a Or reversed.

Table 5. Qualitative correlation between $\delta^{15}\text{N}$ -1 and E_s

R ¹ (compound)	$\delta^{15}\text{N}$ (ppm)	E_s
Me (33)	-217.9	0
Et (34)	-204.2	-0.07
<i>i</i> -Pr (35)	-194.3	-0.47
<i>t</i> -Bu (38)	-188.8	-1.54

2.2.2. ^{13}C NMR chemical shifts. In general, the ^{13}C NMR chemical shifts of the carbon atoms of the flavazole ring system are observed mostly in very narrow ranges for each position. These values are listed in Table 4.

The widest range is shown by C-3. However, its chemical shifts can be grouped in different sets depending on the nature of the substituents in positions 3 and 1. If $\text{R}^3=\text{H}$, the values were found between 131.6 and 135.7 ppm for **3**, **4**, and **30–32**; introducing a carbonyl function into R^1 (**7**) increases the chemical shift to 141.5 ppm. Compounds with $\text{R}^3=\text{Me}$ and no carbonyl function in R^1 show values in the range of 140.4–146.9 ppm; the carbonyl function in R^1 again increases the value to 148.5–149.8 ppm. If chlorine is introduced into position 3, the chemical shifts of this carbon atom were observed in the range of 132.4–133.0 ppm (without a carbonyl containing substituent R^1); the corresponding carbonyl compound (**9**) shows again an increased value of 140.9 ppm. The chemical shifts of C-3 in compounds **10** and **19**, having bromine and CHO at position 3, respectively, were determined to be 130.4 and 140.7 ppm.

The chemical shifts of the carbon atoms in position 3a are in the range of 135.8–138.6 ppm for $\text{R}^3=\text{H}$; halogen or CHO

substitution in position 3 changes it to 132.2–136.2 ppm. The influence of the character of the substituent R^1 is not significant.

Both the quarternary carbons of the phenylene moiety were found to resonate in very narrow ranges: 139.8–142.4 ppm for C-4a, and 140.6–142.5 ppm for C-8a. However, the other carbons of this ring are more separated and resonate in the ranges of 129.7–130.4 ppm for C-5, 126.5–130.4 ppm for C-6, 129.8–132.7 ppm for C-7, and 127.3–129.9 ppm for C-8, respectively. Interestingly, in all investigated compounds the chemical shift of C-5 is downfield from C-8 and that of C-6 is highfield shifted from C-7.

The chemical shifts of C-9a show only a small influence of the substituents R^1 and R^3 , all signals are in the range 141.7–144.7 ppm.

2.2.3. ^{15}N NMR chemical shifts. All measured ^{15}N NMR chemical shifts are given in Table 4.

Due to the varying substitution in position 1 the chemical shift of N-1 shows the widest range (-222.2 to -166.8 ppm). All available substituent constants were tried to be correlated with the N-1 chemical shifts, however only a qualitative correlation between the steric substituent parameter E_s ¹¹ and $\delta^{15}\text{N}$ in the series **33**, **34**, **35**, and **38**, where $\text{R}^3=\text{Me}$ and $\text{R}^1=\text{Me}$, Et, *i*-Pr, and *t*-Bu, respectively, were found (Table 5).

The ^{15}N chemical shifts of N-2 were found in the range of

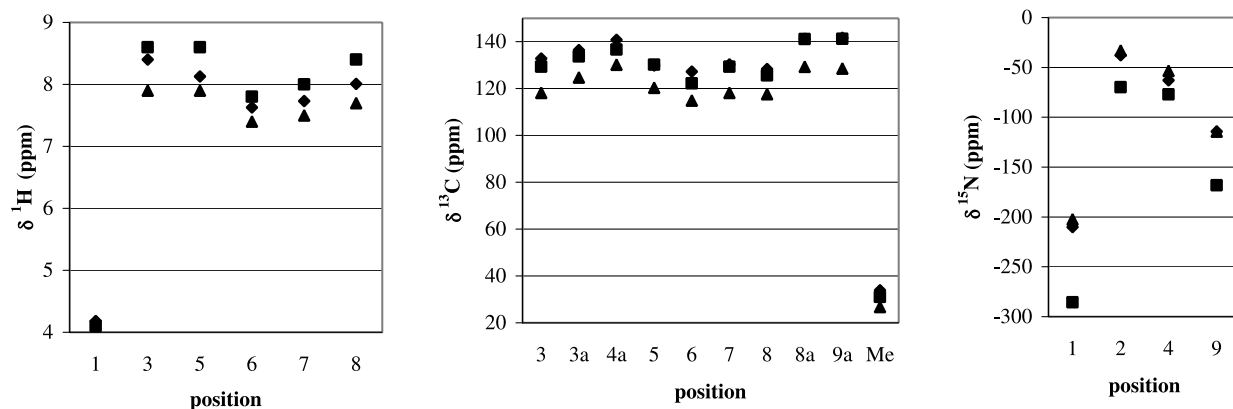


Figure 2. Experimental (\blacklozenge) and calculated (HF/6-31G*: \blacksquare ; B3LYP/6-31G*: \blacktriangle) ^1H , ^{13}C , and ^{15}N chemical shifts of **3**.

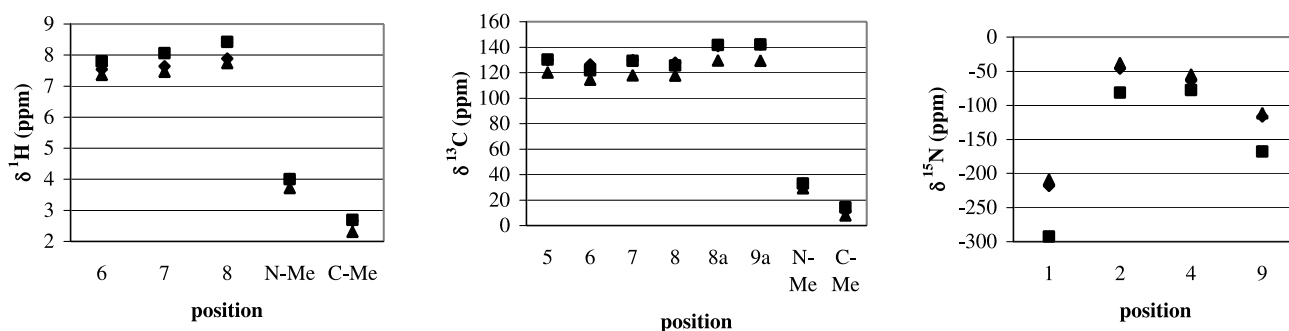


Figure 3. Experimental (\blacklozenge) and calculated (HF/6-31G*: \blacksquare ; B3LYP/6-31G*: \blacktriangle) ^1H , ^{13}C , and ^{15}N chemical shifts of **33**.

Table 6. Calculated and experimental chemical shifts of compounds **34**, **35** and **39**, respectively (ppm)

Atom	Exp.	HF/6-31G*	B3LYP/6-31G*
Compound 34			
H-5	8.12	8.66	7.88
H-6	7.58	7.79	7.36
H-7	7.68	8.05	7.46
H-8	7.98	8.41	7.74
CH ₂	4.53	4.18	4.13
CH ₃ -1	1.56	1.85	1.52
CH ₃ -3	2.75	2.72	2.36
C-3	141.5	139.82	130.27
C-3a	136.0	135.62	125.71
C-4a	140.2	136.16	129.67
C-5	129.9	130.20	120.17
C-6	126.6	121.88	114.58
C-7	130.0	129.11	117.83
C-8	128.1	125.76	117.83
C-8a	141.1	141.48	129.48
C-9a	141.9	142.13	129.48
CH ₂	41.6	37.80	37.06
CH ₃ -1	14.5	12.77	6.93
CH ₃ -3	11.4	14.33	8.34
N-1	-204.2	-283.56	-198.21
N-2	-48.7	-88.00	-46.08
N-4	-64.1	-77.94	-54.91
N-9	-116.6	-167.52	-112.03
Compound 35			
H-5	8.18	8.64	7.87
H-6	7.60	7.77	7.35
H-7	7.71	8.04	7.43
H-8	8.05	8.37	7.70
CH	5.32	5.00	5.04
CH ₃ -1	1.65	1.56	1.30
CH ₃ -3	2.81	2.74	2.38
C-3	141.5	141.21	131.37
C-3a	136.4	134.76	124.89
C-4a	140.5	135.92	129.79
C-5	130.1	130.30	120.16
C-6	126.8	121.61	114.36
C-7	130.1	129.28	117.91
C-8	128.3	125.53	117.61
C-8a	141.3	141.44	129.52
C-9a	141.9	141.49	128.57
CH	48.4	41.63	60.10
CH ₃ -1	21.7	21.92	34.94
CH ₃ -3	11.6	14.49	26.05
N-1	-194.3	-273.16	-188.53
N-2	-52.1	-90.19	-48.39
N-4	-64.1	-77.23	-54.85
N-9	-115.7	-171.25	-115.02
Compound 39			
H-5	8.19	8.65	7.88
H-6	7.63	7.79	7.35
H-7	7.74	8.06	7.46
H-8	8.05	8.38	7.70
-CH ₂ -	5.14	4.82	4.70
-CH=	6.12	6.16	5.75
=CH ₂	5.27	5.52	5.08
CH ₃ -3	2.78	2.70	2.34
C-3	142.5	141.68	132.07
C-3a	136.2	135.22	125.07
C-4a	140.5	135.87	129.58
C-5	130.1	130.30	120.22
C-6	127.0	121.79	114.52
C-7	130.3	129.37	118.04
C-8	128.3	125.50	117.55
C-8a	141.4	141.32	129.49
C-9a	142.4	142.04	129.21
-CH ₂ -	49.1	45.25	44.27
-CH=	132.6	131.48	122.77
=CH ₂	118.0	116.23	107.62
CH ₃ -3	11.5	14.35	8.32
N-1	-208.6	-282.80	-198.62
N-2	-48.0	-83.49	-40.21

Table 6 (continued)

Atom	Exp.	HF/6-31G*	B3LYP/6-31G*
N-4	-63.3	-77.05	-54.48
N-9	-115.5	-171.60	-115.44

-60.7 to -37.1 ppm, whereby the compounds with $R^3 = H$ are situated at the lowfield end, the compounds with $R^3 = Me$ more in the middle, and the compounds with $R^3 =$ halogen at the highfield end of this absorption range. Only **19** with $R^3 = CHO$ is highfield shifted to -29.4 ppm. Successful correlation with common substituent parameters was not observed.

Both, the chemical shifts of N-1 and N-2 are in a comparable range as those found for (substituted) indazoles.¹²

The chemical shifts of N-4 and N-9 show two well separated ranges, which can be used successfully for the unambiguous assignment of the proton and carbon chemical shifts of the phenylene moiety. These ranges are -67.0 to -59.0 ppm for N-4 and -116.6 to -97.9 ppm for N-9. However, an ab initio assignment was only possible for compounds with $R^3 = H$, using the long-range connectivity from H-3 to N-4 from the HMBC experiments. This was corroborated by quantum chemical calculations (see below), which gave also different well separated ranges of the chemical shifts of N-4 and N-9, respectively. Accordingly, it was concluded that where R^3 is other than hydrogen, the chemical shift ranges of N-4 and N-9 do not overlap (Fig. 1).

2.2.4. Quantum chemical calculations. For some of the compounds the ¹H, ¹³C and ¹⁵N chemical shifts were calculated theoretically at different levels of theory (HF/6-31G* and B3LYP/6-31G*). From Figures 2 and 3 and Table 6 it can be concluded that for the ¹H NMR chemical shifts neither of these methods gave significantly better results. In contrast, in case of the ¹³C NMR chemical shifts the HF/6-31G* method and in case of the ¹⁵N NMR chemical shifts the B3LYP/6-31G* method supplied the best results.

The ¹H NMR chemical shifts, especially for the protons of the phenylene moiety, should be influenced by the aromaticity of the flavazole ring system. Therefore, the aromaticity of the different rings were calculated exemplarily for compounds **3**, **4**, **7–10**, **19**, and **33–36**. However, the aromaticity (Table 7) as judged from the calculated chemical shielding of a ghost atom situated 2 Å above the corresponding ring did not show significant differences for the phenyl ring and for the six-membered heterocyclic ring system in the centre of the compounds. The only remarkable deviation was found for the five-membered pyrazole ring system. In this case, the chemical shielding (which was used as an indication of aromaticity) is lowered due to the acetyl group in position 3. However, no significant correlation with the experimental data could be obtained.

Decisive for the unambiguous assignment of the chemical shifts of the phenylene ring nuclei is the unequivocal

Table 7. Calculated chemical shieldings (ppm) of a ghost atom situated 2 Å above the centre of the corresponding ring (A, five-membered pyrazole ring; B, six-membered heterocyclic ring; C, phenylene ring)

Ring	3	4	7-E	7-Z	8-E	8-Z	9-E	9-Z	10-E	10-Z	19-E	19-Z	33	34	35	38
A	4.49	4.52	3.91	3.86	3.72	3.68	3.85	3.80	3.83	3.78	4.12	4.25	4.59	4.50	4.41	4.50
B	6.68	6.69	6.57	6.41	6.48	6.31	6.64	6.48	6.62	6.46	6.49	6.49	6.74	6.69	6.64	6.69
C	5.55	5.56	5.62	5.69	5.63	5.70	5.61	5.69	5.61	5.68	5.44	5.45	5.70	5.56	5.61	5.56

knowledge of the chemical shifts of N-4 and N-9. As already mentioned they could be determined experimentally only for compounds with $R^3=H$. Therefore, special attention was paid to the exact calculation of these chemical shifts. The ^{15}N chemical shifts, thus calculated for **34**, **35**, and **39** (as examples for the whole variety), proved to be different sufficiently to distinguish unequivocally the two nitrogen atoms in the compounds studied. This is surprising because they seem to be very similar. This is why a natural chemical shift (NCS) analysis¹³ was carried out for one case (**35**) which gives the different partitions to the shielding constants from the different chemical bonds, lone pairs, and core electrons. Contributions to the shielding of N-4 and N-9 of major importance are given in Table 8.

Table 8. Most important partitions to the isotropic chemical shielding (ppm) of the nitrogen atoms N-4 and N-9 of **35** as calculated by the NCS analysis

Bond/electron	N-4	Bond/electron	N-9
Core	239.66	Core	239.62
Lone pair N-4	-184.14	Lone pair N-9	-130.2
N-4-C-3a	-60.2	N-9-C-9a	-54.66
N-4-C-4a	-50.2	N-9-C-8a	-48.22
C-3a-C-3	-3.05	C-9a-N-1	-2.65
C-3a-C-9a	-3.46	C-9a-C-3a	-2.74
C-4a-C-5	-2.34	C-8a-C-8	-1.48
C-4a-C-8a	-0.1	C-8a-C-4a	-0.35
Total ^a	-62.96	Total ^a	-2.79

Lewis and non-Lewis contributions are added.

^a Total means of the sum of all partitions to the chemical shieldings of N-4 and N-9, respectively.

As a whole it is found that N-4 is less shielded by about 60 ppm as compared with N-9. This is in good agreement with the experimentally determined values of compound **35** (ca. 52 ppm). From Table 8 it can be seen that the reason for the different chemical shifts of the two nitrogen atoms are the very different contributions of their corresponding N-lone pairs to the shieldings; the other contributions are much more the same.

2.2.5. Restricted rotation about the amide bond. The compounds with $R^1=COMe$ show a splitting of the COMe proton signal at low temperature. This is due to the restricted rotation of the amide bond. Calculated and experimentally detected values of the free energy difference of the rotamers (ΔG°) and the free energy of activation (ΔG^\ddagger) are given in Table 9. The calculated and experimentally determined values of ΔG^\ddagger agree very well; small differences may be due to the inaccuracy of the calculation method. These inaccuracies are probably also the reason for the differences in ΔG° values, which are, however, in this case of higher significance because of their much smaller values compared to ΔG^\ddagger of the rotational isomers.

The rotational barriers (ΔG^\ddagger) for **7–10** are located at the lower end of the range of the free energy of rotation of the amide bond in common amides. Lowering of the barrier in these cases can be caused by a weak basic character of N-1 and by a steric hindrance of the annelated ring system.¹⁴ The theoretical calculations showed that in all cases the (Z)-configuration is more stable than the (E)-analogue. The strong steric hindrance in this part of the molecule should

Table 9. Coalescence temperatures (T_c), free energies (ΔG°), and free energies of activation (ΔG^\ddagger) of the restricted rotation about the amide partial double bond (kJ/mol)

Compound	T_c (K)	ΔG^\ddagger (kJ/mol) ^a	ΔG^\ddagger (kJ/mol) ^{b,c}	ΔG° (kJ/mol) ^a	ΔG° (kJ/mol) ^b
7	235	54.6 and 50.7	46.2	3.43	4.26
8	250	52.9 and 50.0	48.4	2.34	3.76
9	240	48.9 and 46.5	47.5	3.16	3.85
10	240	51.0 and 47.7	47.3	3.52	3.97

Experimental ΔG° was determined at $T=203$ K.

^a Experimental.

^b Calculated with DFT (B3LYP/6-31G*) under consideration of solvent (CD₂Cl₂).

^c Rotation from (*E*) to (*Z*).

also be the reason that no dynamic phenomena of other amidic compounds with a (substituted) benzoyl group at R¹ (**46**, **47**, and **48**, respectively) could be observed. In these cases, obviously one of the two ground states is energetically too unstable to be experimentally detected.

In contrast to the restricted rotation about the amide bond the hindrance of the rotation of the C(O)–C-3 bond in compound **19** could not be observed. The theoretical calculations show a ΔG^\ddagger of 36.3 kJ/mol as barrier of this rotation. Thus, it is much smaller than the energy barrier for the restricted rotation about the amide bond.

2.2.6. Conjugation within 1-phenyl substituted flavazoles. If R¹=Ph, delocalisation of the π electrons of this phenyl ring at N-1 and the flavazole ring system can be expected. As a measure for this conjugation the torsional angle between the two planes of the both aromatic moieties can be considered. For compound **19** it was found by the theoretical calculations to be 0.9 and 2.1° for (*E*) and (*Z*), respectively; so it is more or less planar. The ¹³C NMR chemical shifts of the *o*-carbons and the difference of ¹³C NMR chemical shifts of the *m*- and *o*-carbons of the phenyl moiety were used to assess this interannular conjugation. For an unhindered conjugation in 1-phenyl pyrazoles $\delta(o-C)$ proved to be 118.5–118.8 and the $\delta(m-C)-\delta(o-C)$ 10.5 ppm.¹⁵ The detected values for compounds **15**, **19**, and **30** [$\delta(o-C)$ 119.0–120.2 and $\delta(m-C)-\delta(o-C)$ 8.8–9.8] are much closer to the values of 1-phenyl pyrazole than to the given values obtained in cases of hindered conjugation [$\delta(o-C)$ 124.6–125.4 and $\delta(m-C)-\delta(o-C)$ 3.3–4.0]. Together with the results of the theoretical calculation a non-hindered conjugation along the two aromatic moieties in **15**, **19**, and **30** can be concluded.

3. Experimental

All melting points were determined on a Boetius micro hotstage microscope (Fa. Analytik Dresden). The IR spectra (potassium bromide) were recorded with a Perkin Elmer FTIR 1600 spectrometer (cm⁻¹). The mass spectra were obtained on a Finnigan-MAT SSQ 710 (70 eV). Elemental analyses were performed on the autanalyser CHNS-932 (Fa. Leco Instruments GmbH); reliable microanalyses were obtained for all substances (C, H, N, S \pm 0.3%).

3.1. Syntheses

Compounds **1–4**, **15–17**, and **30–48** were synthesized according to literature.²

3.1.1. General procedure for the synthesis of 3-halo-1H-pyrazolo[3,4-*b*]quinoxalines (5–6). The N-Hal-compound was added slowly to a solution of **1** (50 mmol, 8.50 g) in *N,N*-dimethylformamide (300 mL) at room temperature with stirring. The mixture was heated at 80 °C for 10 min and then 220 mL of the solvent were removed in vacuo. After cooling down to 15 °C the residue was treated with water (100 mL) and kept overnight in the refrigerator. The solid was collected by filtration, washed twice with methanol and recrystallized from xylene or dioxane.

3.1.1.1. 3-Chloro-1H-pyrazolo[3,4-*b*]quinoxaline (5).

From trichloroisocyanuric acid (TCC) (20 mmol, 4.65 g) in 72% yield as yellow prisms, mp 280–281 °C; ms: m/z (%) 207 (20) (M+3)⁺, 206 (36) (M+2)⁺, 205 (60) (M+1)⁺, 204 (100) M⁺, 169 (10) (M-Cl)⁺, 143 (30) (169-CN)⁺, 116 (37) (143-HCN)⁺, 102 (17), 90 (52), 75 (24), 63 (55); IR: 3126, 3038, 2918, 2817, 1716, 1594, 1500, 1480, 1462, 1342, 1294, 1274, 1240, 1202, 1132, 1090, 1036, 968, 916, 852, 800, 768, 728, 606, 544, 460, 436, 420. Elemental analysis (%) for C₉H₅ClN₄: calcd C 52.87, H 2.46, N 27.38; found C 53.11, H 2.50, N 27.40. Because of its extremely low solubility in common solvents no NMR spectra could be taken.

3.1.1.2. 3-Bromo-1H-pyrazolo[3,4-*b*]quinoxaline (6).

From *N*-bromosuccinimide (NBS) (55 mmol, 9.75 g) in 83% yield as yellow as prisms, mp 283–284 °C; ms: m/z (%) 251 (11) (M+3)⁺, 250 (83) (M+2)⁺, 249 (12) (M+1)⁺, 248 (96) M⁺, 169 (50) (M-Br)⁺, 143 (14) (169-CN)⁺, 117 (32) (143-HCN)⁺, 90 (100), 85 (16), 76 (14), 64 (31), 63 (39); IR: 3112, 3022, 2896, 2776, 1716, 1622, 1582, 1500, 1478, 1458, 1424, 1346, 1288, 1270, 1206, 1134, 1086, 1016, 1000, 916, 784, 758, 732, 606, 594, 544, 516, 426. Elemental analysis (%) for C₉H₅BrN₄: calcd C 43.40, H 2.02, N 22.50; found C 43.65, H 2.12, N 22.74. Because of its extremely low solubility in common solvents no NMR spectra could be taken.

3.1.2. General procedure for the acetylation of 1-unsubstituted flavazoles (7–10). The mixture of the appropriate 1-unsubstituted flavazole (10 mmol) and acetic anhydride (25 mL, 265 mmol) was heated under reflux for 30 min and kept overnight in the refrigerator. The solid was collected by filtration under suction, washed with 50% aqueous ethanol and recrystallized.

3.1.2.1. 1-Acetyl-1H-pyrazolo[3,4-*b*]quinoxaline (7).

From **1** in 45% yield as colourless needles (hexane), mp 162–164 °C; ms: m/z (%) 212 (22) M⁺, 211 (100) (M-1)⁺, 210 (95) (M-2)⁺, 169 (20), 168 (85) (M-CH₃CO, -H)⁺,

141 (20) ($M-\text{CH}_3\text{CON}_2$)⁺, 115 (31) (141–CHCH), 74 (6), 62 (8); IR: 3082, 1738, 1577, 1501, 1406, 1380, 1350, 1298, 1256, 1213, 1176, 1134, 1084, 1024, 969, 939, 907, 881, 840, 808, 763, 733, 738, 610, 584, 419. Elemental analysis (%) for $\text{C}_{11}\text{H}_8\text{N}_4\text{O}$: calcd C 62.26, H 3.80, N 26.40; found C 62.45, H 3.82, N 26.52.

3.1.2.2. 1-Acetyl-3-methyl-1H-pyrazolo[3,4-*b*]quinoxaline (8). From **2** in 88% yield as colorless needles (toluene), mp 191–193 °C; ms: *m/z* (%) 226 (9) M^+ , 185 (10), 184 (78) ($M-\text{CH}_2\text{CO}$), 183 (13), 155 (10) (184–HN₂), 143 (54), 116 (18), 102 (17), 90 (10), 76 (11); IR: 3016, 2928, 1846, 1722, 1618, 1580, 1542, 1500, 1446, 1418, 1364, 1312, 1290, 1260, 1246, 1232, 1202, 1148, 1122, 1096, 1038, 1010, 978., 924, 892, 834, 772, 730, 678, 634, 602, 578, 462, 420. Elemental analysis (%) for $\text{C}_{12}\text{H}_{10}\text{N}_4\text{O}$: calcd C 63.71, H 4.46, N 24.77; found C 63.56, H 4.48, N 24.56.

3.1.2.3. 1-Acetyl-3-chloro-1H-pyrazolo[3,4-*b*]quinoxaline (9). From **5** in 62% yield as light brown needles (ethanol), mp 220.5–221.5 °C; ms: *m/z* (%) 248 (8) ($M+2$)⁺, 247 (7) ($M+1$)⁺, 246 (16) M^+ , 206 (32), 205 (12), 204 (100) ($M-\text{CH}_2\text{CO}$)⁺, 169 (17) (204–Cl)⁺, 143 (34), 116 (17), 102 (8), 90 (17), 76 (11), 63 (11); IR: 3062, 2888, 1852, 1747, 1619, 1572, 1498, 1468, 1408, 1374, 1351, 1301, 1281, 1250, 1222, 1188, 1151, 1131, 1066, 969, 918, 873, 836, 775, 725, 663, 630, 602, 571, 547, 420. Elemental analysis (%) for $\text{C}_{11}\text{H}_7\text{ClN}_4\text{O}$: calcd C 53.56, H 2.86, N 22.72; found C 53.61, H 2.86, N 23.01.

3.1.2.4. 1-Acetyl-3-bromo-1H-pyrazolo[3,4-*b*]quinoxaline (10). From **6** in 69% yield as light brown needles (ethanol), mp 220–221 °C; ms: *m/z* (%) 293 (8) ($M+3$)⁺, 292 (21) ($M+2$)⁺, 291 (8) ($M+1$)⁺, 290 (21) M^+ , 251 (9), 250 (100), 248 (84) ($M-\text{CH}_2\text{CO}$), 169 (42) (248–Br)⁺, 143 (12), 117 (12) (143–CN)⁺, 90 (22); IR: 3063, 2934, 1978, 1744, 1565, 1496, 1459, 1409, 1372, 1351, 1296, 1276, 1250, 1216, 1190, 1128, 1058, 964, 916, 858, 835, 761, 727, 627, 573, 520, 419. Elemental analysis (%) for $\text{C}_{11}\text{H}_7\text{BrN}_4\text{O}$: calcd C 45.38, H 2.43, N 19.25. Found C 45.62, H 2.45, N 19.35.

3.1.3. General procedure of alkylation of 3-halo-1H-pyrazolo[3,4-*b*]quinoxalines (11–13). To a solution of 3-halo-1H-pyrazolo[3,4-*b*]quinoxaline (10 mmol) in *N,N*-dimethylformamide (30 mL) the alkylating agent (15 mmol) and powdered anhydrous potassium carbonate (20 mmol, 2.76 g) were added. The mixture was stirred over 24 h at 50 °C and then diluted with water (50 mL). The precipitate was collected by filtration, treated with cold 2 N NaOH, washed with water until neutral and dried.

3.1.3.1. 3-Chloro-1-methyl-1H-pyrazolo[3,4-*b*]quinoxaline (11). From **5** (2.04 g) and methyl iodide (2.13 g) in 57% yield as yellow prisms (dioxane), mp 200–201 °C; ms: *m/z* 220 (26) ($M+2$)⁺, 219 (16) ($M+1$)⁺, 218 (76) M^+ , 217 (19) ($M-1$)⁺, 183 (15) ($M-\text{Cl}$)⁺, 129 (33), 102 (18), 90 (14), 76 (11), 63 (11); IR: 3047, 2940, 1978, 1732, 1574, 1488, 1462, 1400, 1352, 1302, 1242, 1208, 1166, 1116, 1022, 940, 892, 846, 818, 768, 722, 658, 626, 602, 552, 528, 488, 424. Elemental analysis (%) for $\text{C}_{10}\text{H}_7\text{ClN}_4$:

calcd C 54.94, H 3.22, N 25.63; found C 54.93, H 3.19, N 25.81.

3.1.3.2. 3-Chloro-1-ethyl-1H-pyrazolo[3,4-*b*]quinoxaline (12). From **5** (2.04 g) and ethyl iodide (2.33 g) in 56% yield as yellow prisms (hexane), mp 97–99 °C; ms: *m/z* (%) 234 (30) ($M+2$)⁺, 233 (25) ($M+1$)⁺, 232 (100) M^+ , 219 (23), 217 (70) ($M-\text{CH}_3$)⁺, 206 (14), 204 (38) ($M-\text{CH}_2=\text{CH}_2$)⁺, 154 (8), 129 (35), 102 (23), 90 (14); IR: 2986, 2942, 1716, 1652, 1574, 1486, 1460, 1436, 1402, 1378, 1352, 1296, 1238, 1224, 1194, 1166, 1116, 1086, 1046, 982, 928, 882, 846, 794, 764, 724, 650, 618, 602, 554, 488, 424. Elemental analysis (%) for $\text{C}_{11}\text{H}_9\text{ClN}_4$: calcd C 56.78, H 3.90, N 24.08; found C 56.77, H 4.06, N 24.30.

3.1.3.3. 3-Chloro-1-(1-phenylethyl)-1H-pyrazolo[3,4-*b*]quinoxaline (13). From **5** (2.04 g) and (1-bromoethyl)-benzene (2.78 g) in 89% yield as yellow prisms (heptane), mp 128–130 °C; ms: *m/z* (%) 310 (9) ($M+2$)⁺, 309 (5) ($M+1$)⁺, 308 (19) M^+ , 293 (8) ($M-\text{CH}_3$), 207 (5), 206 (28), 205 (19), 204 (100) ($M-\text{C}_6\text{H}_5\text{CHCH}_2$)⁺, 177 (8), 175 (10) ($M-\text{C}_6\text{H}_5\text{CHCH}_2\text{N}_2$)⁺, 169 (12) (204–Cl)⁺, 154 (10) (169–NH)⁺, 143 (22), 129 (16), 116 (23); IR: 3060, 2976, 2930, 2870, 1962, 1716, 1618, 1570, 1496, 1480, 1442, 1404, 1378, 1350, 1298, 1228, 1206, 1176, 1144, 1132, 1118, 1080, 1056, 1030, 1004, 982, 956, 934, 884, 850, 774, 758, 728, 716, 700, 624, 616, 602, 556, 546, 534, 490, 422. Elemental analysis (%) for $\text{C}_{17}\text{H}_{13}\text{ClN}_4$: calcd C 66.13, H 4.24, N 18.15; found C 66.30, H 4.51, N 18.38.

3.1.4. General procedure of halogenation of substituted 1H-pyrazolo[3,4-*b*]quinoxalines (11, 14, 16, 17). The N-Hal-compound was added slowly to a solution of the substituted 1H-pyrazolo [3,4-*b*]quinoxaline (3 mmol) in *N,N*-dimethylformamide (5 mL) at room temperature with stirring. The mixture was heated up to 80 °C and stirred at this temperature for 10 min. After cooling the mixture was diluted with water (5–20 mL). The solid was collected by filtration, washed with a little amount of cold methanol and recrystallized.

3.1.4.1. 3-Chloro-1-methyl-1H-pyrazolo[3,4-*b*]quinoxaline (11). From TCC (1 mmol, 0.23 g) and **3** (0.55 g) in 53% yield as yellow prisms (dioxane), mp 200–201 °C, IR to be identical to the product **11** obtained from 3-chloroflavazole.

3.1.4.2. 3-Bromo-1-tert-butyl-1H-pyrazolo[3,4-*b*]quinoxaline (14). From NBS (3.4 mmol, 0.60 g) and **4** (0.68 g) in 48% yield as yellow needles (ethanol), mp 192–193.5 °C; ms: *m/z* (%) 307 (30) ($M+3$)⁺, 306 (100) ($M+2$)⁺, 305 (30) ($M+1$)⁺, 304 (100) M^+ , 291 (15), 289 (15) ($M-\text{CH}_3$)⁺, 250 (50), 248 (48) ($M-\text{C}_4\text{H}_8$)⁺, 169 (30) (248–Br)⁺, 143 (20), 102 (22), 90 (25); IR: 3068, 2975, 2933, 2683, 1967, 1715, 1622, 1565, 1494, 1477, 1436, 1414, 1388, 1368, 1348, 1292, 1258, 1233, 1198, 1148, 1122, 1068, 1025, 928, 871, 803, 759, 728, 606, 589, 496, 425. Elemental analysis (%) for $\text{C}_{13}\text{H}_{13}\text{BrN}_4$: calcd C 51.16, H 4.29, N 18.36; found C 50.93, H 4.41, N 18.65.

3.1.4.3. 1-(4-Bromophenyl)-3-methyl-1H-pyrazolo[3,4-*b*]quinoxaline (16). Solutions of **15** (2.60 g, 10 mmol) in acetic acid (400 mL) and bromine (1.76 g,

11 mmol) in acetic acid (30 mL) were mixed and kept in a closed bottle for 3 days at room temperature. Thereafter, the mixture was diluted with water (700 mL) and kept in the refrigerator for 24 h. The solid was collected by filtration, washed with water and recrystallized twice from acetic acid. The compound was obtained in 75% yield as yellow needles, mp 241–242°, and found to be identical to the product from 2-acetylquinoxaline oxime and 4-bromophenylhydrazine.² Because of its extreme bad solubility in common solvents no NMR spectra could be recorded.

3.1.4.4. 1-(4-Chlorophenyl)-3-methyl-1H-pyrazolo[3,4-*b*]quinoxaline (17). From TCC (1 mmol, 0.23 g) and **15** (0.78 g) in 50% yield as yellow needles (toluene), mp 234–236 °C, IR is identically with the product from 2-acetylquinoxaline oxime and 4-chlorophenylhydrazine.² Because of its extreme bad solubility in common solvents no NMR spectra could be recorded.

3.1.4.5. 1-Phenyl-1H-pyrazolo[3,4-*b*]quinoxalin-3-carbaldehyde (19). A solution of **18**¹⁶ (10 mmol, 3.36 g) in hot dioxane (200 mL) was slowly poured into a suspension of KIO₄ (25 mmol, 5.75 g) and NaHCO₃ (30 mmol, 2.52 g) in 1 kg ice-water under vigorous stirring. The mixture was allowed to warm up to room temperature in 1 h and stirring was continued for 2–4 h. The mixture was kept overnight in the refrigerator. The solid was collected by filtration and washed with water. The crude product was considerably pure. The yield was 2.60 g (95%) yellow-brown prisms, mp 143.5–144.5 °C, after recrystallization from ethanol 2.10 g (77%) golden prisms, mp 145–146 °C; ms: *m/z* (%) 276 (12) (M+2)⁺, 275 (65) (M+1)⁺, 274 (100) M⁺, 246 (14), 245 (64) (M-CHO), 219 (6), 218 (9) (245-HCN)⁺, 77 (7) C₆H₅; IR: 3043, 3063, 2867, 2829, 1939, 1793, 1699, 1593, 1568, 1498, 1465, 1430, 1397, 1375, 1359, 1331, 1322, 1292, 1237, 1205, 1149, 1069, 1027, 1008, 996, 959, 934, 901, 891, 856, 847, 834, 802, 767, 743, 688, 669, 648, 614, 600, 536, 506, 481, 425. Elemental analysis (%) for C₁₆H₁₀N₄O: calcd C 70.06, H 3.67, N 20.43; found C 70.22, H 3.59, N 20.27.

3.1.4.6. (1-Phenyl-1H-pyrazolo[3,4-*b*]quinoxalin-3-carbaldehyde)-(*p*-tolylsulfonyl)hydrazone (20). A mixture of the carbaldehyde **19** (2.74 g, 10 mmol), *p*-toluenesulfonyl hydrazide (2.05 g, 11 mmol) and ethanol (300 mL) was heated under reflux for 30 min, in which time the hydrazone began to crystallize. The product was allowed to stand overnight in the refrigerator. The solid was collected by suction filtration. The compound was obtained in 56% yield after recrystallization as orange prisms (1-butanol), mp 205–207 °C (dec.); ms: *m/z* (%) 443 (M+1)⁺, 287 (19) (M-CH₃C₆H₄SO₂), 260 (20), 259 (100) (287-N₂)⁺, 258 (13), 156 (17) (M-287+H)⁺, 139 (15) (156-OH)⁺, 102 (12), 92 (17), 91 (31), 77 (36), 65 (18); IR: 3442, 3190, 3046, 2923, 2860, 2794, 1936, 1597, 1567, 1499, 1450, 1425, 1349, 1303, 1293, 1242, 1207, 1184, 1165, 1092, 1078, 1041, 967, 920, 910, 885, 852, 818, 801, 784, 759, 706, 690, 673, 658, 595, 566, 546, 531, 498, 475, 421. Elemental analysis (%) for C₂₃H₁₈N₆O₂S: calcd C 62.43, H 4.10, N 18.99; found C 62.25, H 4.01, N 19.18. Because of its extremely low solubility in common solvents no NMR spectra could be taken.

3.1.5. General procedure for aminomethylation of 1H-pyrazolo[3,4-*b*]quinoxalines (21–29). To a suspension of **2** (10 mmol, 1.84 g) in ethanol (20 mL), an appropriate amine (12 mmol) and finally formalin (1.2 mL, 16 mmol) [solution of 37% CH₂=O in water] were added under stirring. The reaction was weakly exothermic (the temperature increased from 25 °C until 29 °C). The mixture was then heated under reflux for 2–5 min till the product began to crystallize. The mixture was kept overnight in the refrigerator. The solid was collected by filtration, washed with cold 2 N NaOH (if not esters), and with water or diluted ethanol. The products were purified by recrystallization.

3.1.5.1. 1-Diethylaminomethyl-3-methyl-1H-pyrazolo[3,4-*b*]quinoxaline (21). From diethyl amine in 48% yield as yellow needles (hexane), mp 75.5–76.5 °C; ms: *m/z* (%) 270 (6) (M+1)⁺, 269 (1.5) M⁺, 213 (21), 212 (86) (M-C₂H₅-C₂H₄)⁺, 197 (29) (M-Et₂N)⁺, 129 (30) (C₆H₄NC₃H₃)⁺, 102 (24), 87 (35), 86 (100) (Et₂NCH₂)⁺, 58 (31); IR: 3066, 2964, 2926, 2822, 1958, 1576, 1498, 1480, 1476, 1380, 1350, 1334, 1308, 1240, 1216, 1200, 1172, 1134, 1118, 1090, 1062, 1022, 996, 978, 952, 898, 842, 802, 758, 730, 708, 640, 616, 602, 554, 424. Elemental analysis (%) for C₁₅H₁₉N₅: calcd C 66.89, H 7.11, N 26.00; found C 66.75, H 6.98, N 25.92.

3.1.5.2. 1-Diisobutylaminomethyl-3-methyl-1H-pyrazolo[3,4-*b*]quinoxaline (22). From diisobutyl amine in 75% yield as yellow needles (heptane), mp 101.5–102.5 °C; ms: *m/z* (%) 326 (5) (M+1)⁺, 282 (21) (M-CH₃CHCH₃), 241 (20), 240 (82) (M-CH₂=C-CH₃), 198 (29), 197 (91), 143 (55), 142 (100) (M-CH₃CN: 2=C₈H₄N₃+C₉H₂₀N)⁺, 129 (70), 128 (23), 102 (31), 100 (20), 98 (19), 86 (37), 57 (54) (CH₂CH(CH₃)₂)⁺; IR: 3040, 2964, 2866, 2826, 1946, 1728, 1632, 1578, 1498, 1482, 1466, 1404, 1382, 1356, 1352, 1308, 1282, 1244, 1204, 1170, 1120, 1078, 1018, 970, 954, 930, 900, 848, 822, 766, 726, 706, 646, 616, 602, 558, 424. Elemental analysis (%) for C₁₉H₂₇N₅: calcd C 70.12, H 8.36, N 21.57; found C 70.05, H 8.30, N 21.44.

3.1.5.3. 3-Methyl-1-pyrrolidinomethyl-1H-pyrazolo[3,4-*b*]quinoxaline (23). From pyrrolidine in 83% yield as yellow needles (heptane), mp 137–139 °C; ms: *m/z* (%) 268 (21) (M+1)⁺, 267 (41) M⁺, 199 (13), 198 (71), 197 (22) (M-pyrrolidino)⁺, 129 (23), 102 (19), 85 (32), 84 (100), 83 (18), 70 (47) pyrrolidino⁺, 55 (27); IR: 3064, 2938, 2874, 2830, 1938, 1716, 1576, 1498, 1478, 1458, 1386, 1344, 1310, 1272, 1242, 1150, 1116, 1084, 1024, 980, 962, 900, 842, 754, 722, 648, 606, 588, 520, 420. Elemental analysis (%) for C₁₅H₁₇N₅: calcd C 67.39, H 6.41, N 26.20; found C 67.47, H 6.44, N 26.48.

3.1.5.4. 3-Methyl-1-piperidinomethyl-1H-pyrazolo[3,4-*b*]quinoxaline (24). From piperidine in 87% yield as yellow needles (heptane), mp 120–121 °C; ms: *m/z* (%) 282 (23) (M+1)⁺, 281 (66) M⁺, 198 (58), 197 (55) (M-piperidino)⁺, 185 (42), 155 (17), 143 (10), 129 (55), 128 (10), 102 (27), 98 (100) [CH₂N(CH₂)₅]⁺, 96 (27), 84 (10) piperidino⁺, 55 (20); IR: 3040, 2936, 2852, 2810, 2762, 1618, 1580, 1558, 1514, 1498, 1480, 1452, 1404, 1386, 1348, 1328, 1310, 1285, 1248, 1170, 1136, 1118, 1062, 1022, 996, 978, 948, 902, 852, 842, 764, 728, 716, 648, 618, 604, 584, 552, 520, 482, 424. Elemental analysis (%) for

$C_{16}H_{19}N_5$: calcd C 68.30, H 6.81, N 24.89; found C 68.52, H 6.93, N 25.12.

3.1.5.5. 3-Methyl-1-morpholinomethyl-1H-pyrazolo[3,4-b]quinoxaline (25). From morpholine in 60% yield as yellow needles (ethanol), mp 186.5–187.5 °C; ms: m/z (%) 284 (3.4) (M+1)⁺, 283 (17) M⁺, 199 (17), 198 (61), 197 (13) (M–morpholino)⁺, 129 (13), 101 (16), 100 (100) [CH₂N(C₂H₄)₂O]⁺, 86 (15) morpholino⁺, 56 (34); IR: 3062, 2968, 2938, 2914, 2853, 2826, 1918, 1806, 1700, 1612, 1578, 1498, 1478, 1448, 1434, 1384, 1366, 1338, 1310, 1264, 1240, 1208, 1170, 1150, 1138, 1116, 1100, 1070, 1006, 976, 892, 862, 842, 798, 774, 754, 726, 650, 618, 608, 556, 528, 502, 424. Elemental analysis (%) for C₁₅H₁₇N₅O: calcd C 63.59, H 6.05, N 24.72; found C 63.33, H 6.16, N 24.17.

3.1.5.6. Ethyl 1-(3-methyl-1H-pyrazolo[3,4-b]quinoxalin-1-ylmethyl)piperidin-4-carboxylate (26). From ethyl piperidin-4-carboxylate in 91% yield as golden needles (heptane), mp 133–134 °C; ms: m/z (%) 354 (7) (M+1)⁺, 353 (16) M⁺, 308 (10) (M–C₂H₅O)⁺, 198 (25), 197 (22) (M–156)⁺, 171 (31), 170 (100) (197–HCN)⁺, 169 (10), 157 (11), 156 (87) (M–197 or 170–CH₂ or 197–CH₃CN)⁺, 142 (35) (170–CH₂N or 170–CH₂=CH₂), 129 (21), 99 (23), 97 (12), 96 (20); IR: 2940, 2804, 2764, 1724, 1580, 1556, 1510, 1496, 1480, 1444, 1402, 1370, 1348, 1326, 1308, 1268, 1254, 1244, 1176, 1144, 1198, 1044, 1024, 998, 968, 952, 902, 864, 840, 766, 714, 648, 620, 602, 584, 552, 422. Elemental analysis (%) for C₁₉H₂₃N₅O₂: calcd C 64.57, H 6.56, N 19.82; found C 64.41, H 6.47, N 19.95.

3.1.5.7. 3-Methyl-1-(4-methylpiperazin-1-yl)methyl-1H-pyrazolo[3,4-b]quinoxaline (27). From 1-methylpiperazine in 62% yield as yellow needles (heptane), mp 143–144 °C; ms: m/z (%) 298 (6) (M+2)⁺, 297 (20) (M+1)⁺, 296 (13) M⁺, 197 (18) (M–methylpiperazine)⁺, 129 (15), 114 (15), 113 (89) [CH₂N(C₂H₄)₂NCH₃]⁺, 112 (36), 111 (100) (113–2H), 102 (16); IR: 3052, 2962, 2938, 2880, 2828, 2794, 2764, 1580, 1514, 1500, 1450, 1406, 1386, 1350, 1326, 1312, 1286, 1234, 1200, 1170, 1146, 1120, 1072, 1052, 1010, 976, 902, 800, 768, 736, 724, 654, 618, 554, 526, 424. Elemental analysis (%) for C₁₆H₂₀N₆: calcd C 64.84, H 6.80, N 28.36; found: C 64.71, H 6.53, N 28.18.

3.1.5.8. Ethyl 4-(3-methyl-1H-pyrazolo[3,4-b]quinoxalin-1-ylmethyl)piperazin-1-carboxylate (28). From ethyl piperazin-1-carboxylate in 81% yield as yellow needles (heptane), mp 165–166 °C; ms: m/z (%) 355 (3.9) (M+1)⁺, 354 (11) M⁺, 199 (10), 198 (50), 197 (19) [M–N(C₂H₄)₂NCOOEt]⁺, 172 (21), 171 (100) [CH₂N(C₂H₄)₂NCOOEt]⁺, 170 (11), 169 (32), 157 (39) (M–197), 143 (28), 129 (40), 102 (24), 98 (14), 97 (29), 70 (28), 56 (41), 55 (13); IR: 3060, 2978, 2952, 2832, 1682, 1580, 1516, 1498, 1480, 1460, 1432, 1386, 1374, 1362, 1340, 1310, 1282, 1244, 1211, 1176, 1156, 1118, 1100, 1080, 1028, 1004, 962, 876, 842, 766, 732, 722, 654, 618, 602, 590, 554, 540, 422. Elemental analysis (%) for C₁₈H₂₂N₆O₂: calcd C 61.00, H 6.26, N 23.71; found C 60.87, H 6.22, N 23.52.

3.1.5.9. 1-[N-(2-Chloropyrid-5-ylmethyl)-N-methylamino]methyl-3-methyl-1H-pyrazolo-[3,4-b]-quinoxaline (29). From 2-chloro-5-(N-methylaminomethyl)pyridine

as yellow needles (ethanol), mp 113–115 °C; ms: m/z (%) 354 (1.9) (M+2)⁺, 353 (4.2) (M+1)⁺, 352 (3.8) M⁺, 309 (13), 199 (13), 198 (95) (M–CH₃NCHPyCl)⁺, 197 (16), 171 (90) (CH₃N(CH₂)CH₂Py³⁷Cl)⁺, 169 (100) (CH₃N(CH₂)CH₂Py³⁵Cl)⁺, 155 (13) (M–198)⁺, 129 (25), 128 (65), 126 (95), 102 (24), 99 (11), 90 (20); IR: 3050, 2982, 2946, 2846, 2814, 1626, 1590, 1584, 1516, 1494, 1458, 1384, 1358, 1322, 1308, 1224, 1168, 1134, 1106, 1040, 1016, 974, 948, 916, 850, 816, 758, 720, 682, 640, 616, 602, 558, 494, 452, 420. Elemental analysis (%) for C₁₈H₁₇ClN₆: calcd C 61.28, H 4.86, N 23.82; found C 61.42, H 5.08, N 24.05.

3.2. NMR measurements

NMR spectra were recorded using Bruker Avance 500 or Avance 300 spectrometers. For preparing the solutions 130–160 mg (in case of good solubility) were dissolved in 0.7 mL of chloroform-d. If the solubility was not good enough saturated solutions were used. Chemical shifts were referenced to TMS (for ¹H), to the solvent (¹³C), or to external CH₃NO₂ (=0 ppm for ¹⁵N). In some cases it was not possible to get 1D ¹⁵N spectra, here the chemical shifts were extracted from the 2D ¹H, ¹⁵N-gs-HMBC spectra. All 1D and 2D COSY, HMQC, and HMBC experiments were taken from the standard Bruker software. To measure heteronuclear long-range J couplings pulse sequences described in literature^{8,9} were used.

Low-temperature ¹H NMR measurements were done on solutions of ca. 20 mg in 0.7 mL of CD₂Cl₂. The free energies of rotation (ΔG^\ddagger) were calculated by the method of Shanan-Atidi and Bar-Eli¹⁷ using the methyl signals of the acetyl group.

3.3. Quantum chemical calculations

The ab initio program package GAUSSIAN 98¹⁸ was used for all calculations which were carried out at the Hartree-Fock and DFT-B3LYP¹⁹ level by means of 6-31G* split-valence basis set.²⁰ The geometry optimization of selected compounds was performed without restrictions. The quantum-chemical calculations were processed on SGI Octane and a Linux cluster at Potsdam University.

The magnetic shieldings of all nuclei were calculated using the GIAO method²¹ implemented in GAUSSIAN 98 at the theory level mentioned above. The chemical shifts are differences in magnetic shielding of atoms and references. As references for ¹³C and ¹H TMS, for ¹⁵N chemical shifts nitromethane were employed.

The NBO 5.0¹³ was used to link the GAUSSIAN 98 program. The natural chemical shielding (NCS)-NBO analysis partitions quantitatively the magnetic shielding of a certain nucleus into magnetic contributions from core orbitals (major), chemical bond and lone pair orbitals. The shielding and deshielding contributions are divided into Lewis and non-Lewis parts. Non-Lewis parts are connected with electron density in antibonding orbitals.

Supplementary data

Supplementary data associated with this article can be found, in the online version, at doi:10.1016/j.tet.2005.01.013; or is available on request.

References and notes

1. Part XIII: Starke, I.; Sarodnick, G.; Ovcharenko, V. V.; Pihlaja, K.; Kleinpeter, E. *Tetrahedron* **2004**, *60*, 6063–6078. Part XII: Sarodnick, G.; Heydenreich, M.; Linker, T.; Kleinpeter, E. *Tetrahedron* **2003**, *59*, 6311–6321.
2. Sarodnick, G.; Linker, T. *J. Heterocyclic Chem.* **2001**, *38*, 829–836.
3. Monge, A.; Palop, J. A.; Pinol, A.; Martinez-Crespo, F. J.; Narro, S.; Gonzales, M.; Sainz, Y.; Lopez de Cerain, A.; Hamilton, E.; Barker, A. I. *J. Heterocyclic Chem.* **1994**, *31*, 1135–1139.
4. Ohle, H.; Melkonian, G. A. *Ber. Dtsch. Chem. Ges.* **1941**, *74*, 398–408.
5. El-Maghraby, M. A.; Koraiem, A. I. M.; Khalil, Z. H.; El-Hamed, R. M. A. *Indian J. Chem.* **1987**, *26B*, 52–54.
6. Ohle, H.; Melkonian, G. A. *Ber. Dtsch. Chem. Ges.* **1941**, *74*, 279–291.
7. Buu-Hoi, N. P.; Vallat, J.-N.; Saint-Ruf, G.; Lambelin, G. *Chim. Ther.* **1971**, 245–250. **1972**, 210–213.
8. Braun, S.; Kalinowski, H.-O.; Berger, S. *150 and More Basic NMR Experiments*; Wiley-VCH: Weinheim, 1998; p 241.
9. Furihata, K.; Seto, H. *Tetrahedron* **1999**, *4*, 6271.
10. Heydenreich, M.; Koch, A.; Kovács, J.; Tóth, G.; Kleinpeter, E. *Magn. Reson. Chem.* **2004**, *42*, 667–670.
11. Exner, O. In *Correlation Analysis in Chemistry*; Chapman, N. B., Shorter, J., Eds.; Plenum: New York, 1978; p 526 ff.
12. Claramunt, R. M.; Sanz, D.; Lopez, C.; Jimenez, J. A.; Jimeno, M. L.; Elguero, J.; Fruchier, A. *Magn. Reson. Chem.* **1997**, *35*, 35–75.
13. NBO 5.0, Glendening, E. D.; Badenhoop, J. K.; Reed, A. E.; Carpenter, J. E.; Bohmann, J. A.; Morales, C. M.; Weinhold, F. Theoretical Chemistry Institute, University of Wisconsin, Madison 2001. Bohmann, J. A.; Weinhold, F.; Farrar, T. C. *J. Chem. Phys.* **1997**, *107*, 1173–1184.
14. Oki, M. *Applications of Dynamic NMR Spectroscopy to Organic Chemistry*; VCH: Deerfield Beach, 1985; pp 43 ff.
15. Begtrup, M. *Acta Chem. Scand.* **1974**, *B28*, 61–77.
16. Weygand, F.; Fehr, K.; Klebe, J. F. *Z. Naturforsch.* **1959**, *14B*, 217–220.
17. Shanan-Atidi, H.; Bar-Eli, K. *J. Phys. Chem.* **1970**, *74*, 961–963.
18. Gaussian 98 (Revision A.12), Frisch, M. J.; Trucks, G. W.; Schlegel, H. B.; Scuseria, G. E.; Robb, M. A.; Cheeseman, J. R.; Zakrzewski, V. G.; Montgomery, J. A., Jr.; Stratmann, R. E.; Burant, J. C.; Dapprich, S.; Millam, J. M.; Daniels, A. D.; Kudin, K. N.; Strain, M. C.; Farkas, O.; Tomasi, J.; Barone, V.; Cossi, M.; Cammi, R.; Mennucci, B.; Pomelli, C.; Adamo, C.; Clifford, S.; Ochterski, J.; Petersson, G. A.; Ayala, P. Y.; Cui, Q.; Morokuma, K.; Rega, N.; Salvador, P.; Dannenberg, J. J.; Malick, D. K.; Rabuck, A. D.; Raghavachari, K.; Foresman, J. B.; Cioslowski, J.; Ortiz, J. V.; Baboul, A. G.; Stefanov, B. B.; Liu, G.; Liashenko, A.; Piskorz, P.; Komaromi, I.; Gomperts, R.; Martin, R. L.; Fox, D. J.; Keith, T.; Al-Laham, M. A.; Peng, C. Y.; Nanayakkara, A.; Challacombe, M.; Gill, P. M. W.; Johnson, B.; Chen, W.; Wong, M. W.; Andres, L.; Gonzalez, C.; Head-Gordon, M.; Replogle, E. S.; Pople, J. A. *Gaussian*, Pittsburgh, PA, 2002.
19. Becke, A. D. *J. Chem. Phys.* **1993**, *98*, 1372–1377.
20. Hehre, W. J.; Radom, L.; Schleyer, P. v. R.; Pople, J. A. *Ab Initio Molecular Orbital Theory*; Wiley: New York, 1986.
21. Ditchfield, R. *Mol. Phys.* **1974**, *27*, 789–807. Cheeseman, J. R.; Trucks, G. W.; Keith, T. A.; Frisch, M. J. *J. Chem. Phys.* **1996**, *104*, 5497–5509.